Human Molecular Genetics, 2014, Vol. 23, No. 3 **563–577**
doi:10.1093/hmg/ddt445
Advance Access published on September 18, 2013

The coiled-coil domain containing protein CCDC151 is required for the function of IFT-dependent motile cilia in animals

Julie Jerber[1], Dominique Baas[2], Fabien Soulavie[1], Brigitte Chhin[1], Elisabeth Cortier[1], Christine Vesque[3,4], Joëlle Thomas[1,†] and Bénédicte Durand[1,†,*]

[1]Centre de Génétique et de Physiologie Moléculaire et Cellulaire, UMR 5534 CNRS, Université Claude Bernard Lyon 1, Villeurbanne 69622, France, [2]Equipe Différenciation Neuromusculaire, Laboratoire de Biologie Moléculaire de la Cellule, CNRS UMR 5239/ENS Lyon, Université de Lyon, IFR128 Biosciences Lyon-Gerland, 46, allée d'Italie, 69364 Lyon cedex 07, France, [3]Centre National de la Recherche Scientifique (CNRS) UMR 7622, Institut National de la Santé et de la Recherche Médicale (INSERM) U969, Paris 75005, France and [4]Université Pierre et Marie Curie, Paris 75005, France

Received July 11, 2013; Revised September 4, 2013; Accepted September 7, 2013

Cilia are evolutionarily conserved organelles endowed with essential physiological and developmental functions. In humans, disruption of cilia motility or signaling leads to complex pleiotropic genetic disorders called ciliopathies. Cilia motility requires the assembly of multi-subunit motile components such as dynein arms, but mechanisms underlying their assembly pathway and transport into the axoneme are still largely unknown. We identified a previously uncharacterized coiled-coil domain containing protein CCDC151, which is evolutionarily conserved in motile ciliated species and shares ancient features with the outer dynein arm-docking complex 2 of *Chlamydomonas*. In *Drosophila*, we show that CG14127/CCDC151 is associated with motile intraflagellar transport (IFT)-dependent cilia and required for geotaxis behavior of adult flies. In zebrafish, Ccdc151 is expressed in tissues with motile cilia, and morpholino-induced depletion of Ccdc151 leads to left–right asymmetry defects and kidney cysts. We demonstrate that Ccdc151 is required for proper motile function of cilia in the Kupffer's vesicle and in the pronephros by controlling dynein arm assembly, showing that Ccdc151 is a novel player in the control of IFT-dependent dynein arm assembly in animals. However, we observed that CCDC151 is also implicated in other cellular functions in vertebrates. In zebrafish, *ccdc151* is involved in proper orientation of cell divisions in the pronephros and genetically interacts with *prickle1* in this process. Furthermore, knockdown experiments in mammalian cells demonstrate that CCDC151 is implicated in the regulation of primary cilium length. Hence, CCDC151 is required for motile cilia function in animals but has acquired additional non-motile functions in vertebrates.

INTRODUCTION

Cilia or flagella are highly conserved structures implicated in fundamental functions from protozoa to mammals. Cilia are involved in cell and fluid motility and serve sensory and signaling functions. Cilia or flagella are built around a core microtubule skeleton composed of nine microtubule doublets, with additional features varying between motile and sensory cilia. In motile cilia, specific components are observed and required for motility, which includes inner dynein arms (IDA) and outer dynein arms, nexin links and most often a central pair of microtubules linked to the peripheral doublets by radial spokes.

In humans, cilia dysfunction leads to various syndromes with complex symptoms that can be due to defects either in cilia motility or in signaling (1,2). Defects in cilia motility lead to a characteristic pathology called primary ciliary dyskinesia (PCD). Whereas 21 genes (*DNAH5, DNAH11, DNAI1, DNAI2, TXNDC3, DNAL1, CCDC103, CCDC114, KTU, LRRC50,*

*To whom correspondence should be addressed at: CGphiMC UMR 5534, Université Lyon-1, Bâtiment Gregor Mendel, 16 rue Dubois, 69622 Villeurbanne, France. Tel: +33 472431326; Fax: +33 472432685; Email: benedicte.durand@univ-lyon1.fr
†Co-senior authors.

LRRC6, HEATR2, DNAAF3, RPGR, OFD1, RSPH9, RSPH4A, HYDIN, CCDC39, CCDC40, CCDC164) responsible for this disease have already been described, many remain to be identified to explain all PCD cases (3). A majority of the genes identified to date are involved in the assembly of axonemal dynein arms or motile features such as radial spokes or the central pair of microtubules. Studies in *Chlamydomonas* provided essential information on the components required for cilia motility. A mutagenesis screen for paralyzed or slowed flagella allowed the characterization of several classes of mutants affecting different structures of the axoneme such as axonemal dynein arms (4). This led to the identification of several components of the axonemal dynein complexes or assembly pathway (reviewed in 5). In addition, genetic studies in zebrafish and human ciliopathies uncovered novel components of the assembly pathway and yielded insights into its conservation throughout evolution (6–12; reviewed in 13).

Dynein arm assembly is initiated in the cytoplasm and requires at least three dynein assembly factors, DNAAF1 to 3, which, when mutated, give rise to PCD in humans (7,10,14,15). Dynein arms are then transported along the axoneme by the intraflagellar transport (IFT) machinery. A few proteins playing a specific role in the transport of motile components have been described. For example, ODA16/WDR69 is a protein specifically required for the assembly of outer dynein arms and directly interacts with the IFT machinery (16,17). Outer dynein arms were shown to be transported by IFT46 into *Chlamydomonas* flagella (18). Attachment of dynein arms to the microtubule templates requires the dynein docking complex, first described in *Chlamydomonas*. In the green algae, at least three proteins—DC1/ODA3, DC2/ODA1 and DC3/ODA14—were identified as components of the outer dynein arm-docking complex that interact with both tubulin and dynein arms (19–22). In humans, mutations in the ODA1/DC2 component CCDC114 lead to PCD (11,12). Several other proteins are required for the recruitment of dynein arms to the axonemes, such as the ODA5/ODA8/ODA10 complex identified in *Chlamydomonas* (23). In addition, two coiled-coil proteins—CCDC39 and CCDC40—emerged from studies of PCD patients, dog and zebrafish mutants (8,9). These proteins function in the assembly of IDA. Recently, mutations in the gene encoding CCDC103 were found in PCD patients and this protein was shown to be tightly bound to the axoneme and required for IDA and outer dynein arms attachment (6). Finally, CCDC164, identified in *Chlamydomonas* and humans as a component of the dynein regulatory complex (DRC, or nexin link), is also involved in PCD (24).

Despite this growing number of data on actors of cilia motility, several aspects of the dynein assembly pathway are not understood. Evidence suggests the existence of still unidentified IFT cargoes required to transport dynein arms or components of the DRCs into the axoneme (16). The specificity and coordination of the outer dynein arm versus IDA transport constitute another important and unresolved issue. In non-motile cilia, adapters seem to exist to couple specific ciliary cargoes to IFT, thus playing an important role in the regulation of cilium length and ciliary signal transduction (reviewed in 25,26).

We show here that CCDC151, initially identified as a target gene of the ciliogenic transcription factor RFX in *Drosophila* (27), is an evolutionarily conserved protein that is specific to species with motile cilia. CCDC151 shares ancestral features with ODA1/DC2 from *Chlamydomonas* and with several members of the ODA1 family of proteins in mammals that includes CCDC114 and CCDC63 in mice and humans. In *Drosophila*, we show that CG14127/CCDC151 is specifically associated with motile IFT-dependent sensory cilia but not with flagellar axonemes that do not require IFT for their assembly (28–30). This suggests that CCDC151 is not a structural component of the motile axoneme in *Drosophila*. In zebrafish, we show that *ccdc151* is strongly expressed in motile ciliated tissues, where it is required for dynein arm assembly and for the transport of the docking complex CCDC114. These results identify CCDC151 as a novel regulator of motile cilia function. In addition, we show that the function of CCDC151 is not restricted to cilia motility. Indeed, we demonstrate in zebrafish that *ccdc151* is also involved in the control of cell division orientations and functionally interacts with the planar cell polarity (PCP) pathway component *prickle1* in this process. Moreover, knockdown of *Ccdc151* in IMCD3 mouse cells results in a deregulated ciliary length. These results prompt us to propose that CCDC151 has a more general function related to IFT-dependent transport of ciliary components.

RESULTS

CCDC151 is evolutionarily conserved in motile ciliated species

We previously identified *CG14127* as an X-Box-containing gene in *Drosophila*, suggesting a potential ciliary function (27). CG14127 and CCDC151 orthologs in vertebrates belong to a coiled-coil family of proteins related to ODA1/DC2, a docking complex protein (5,11,12,20), and ODA5 (23), both involved in the assembly of outer dynein arms in *Chlamydomonas*. Two subgroups can be distinguished in the family (Fig. 1A): (i) the first one includes CG14127 and its CCDC151 orthologs in vertebrates and CCDC151 paralogs (KIAA1984) in mammals; (ii) the second one contains two *Drosophila* genes: CG14905 and CG17083 and their orthologs in mammals, CCDC63 and CCDC114, the latter being involved in dynein arm assembly in humans (11,12). Only one ortholog, Ccdc114, is present in zebrafish. Even though these two subgroups share ancient features with *Chlamydomonas* ODA1 or ODA5, the best reciprocal hit of ODA1 or ODA5 in *Drosophila* is CG14905 from the second subgroup and not CG14127 from the CCDC151 subgroup. Both subgroups have likely evolved separately. Whereas observations in humans show that CCDC114 has conserved a function in docking dynein arms to the axoneme, no functional data exist for the CCDC151 subgroup.

We examined the conserved domains of CCDC151 proteins from humans, mice, zebrafish and *Drosophila* by alignments of the protein sequences (Supplementary Material, Fig. S1) and determined the position of the conserved coiled-coil domains (Fig. 1B). Next, we searched for CCDC151 occurrence in various ciliated species and found potential orthologs only in species with motile cilia (Fig. 1C). For example, no ortholog could be identified in *Caenorhabditis elegans*, which lacks motile cilia, whereas members of the ODA1 family were identified in various ciliated protozoa species such as *Tetrahymena thermophila* (Fig. 1A and C). No ortholog was found in *Plasmodium falciparum*, in which motile flagella assembly takes place

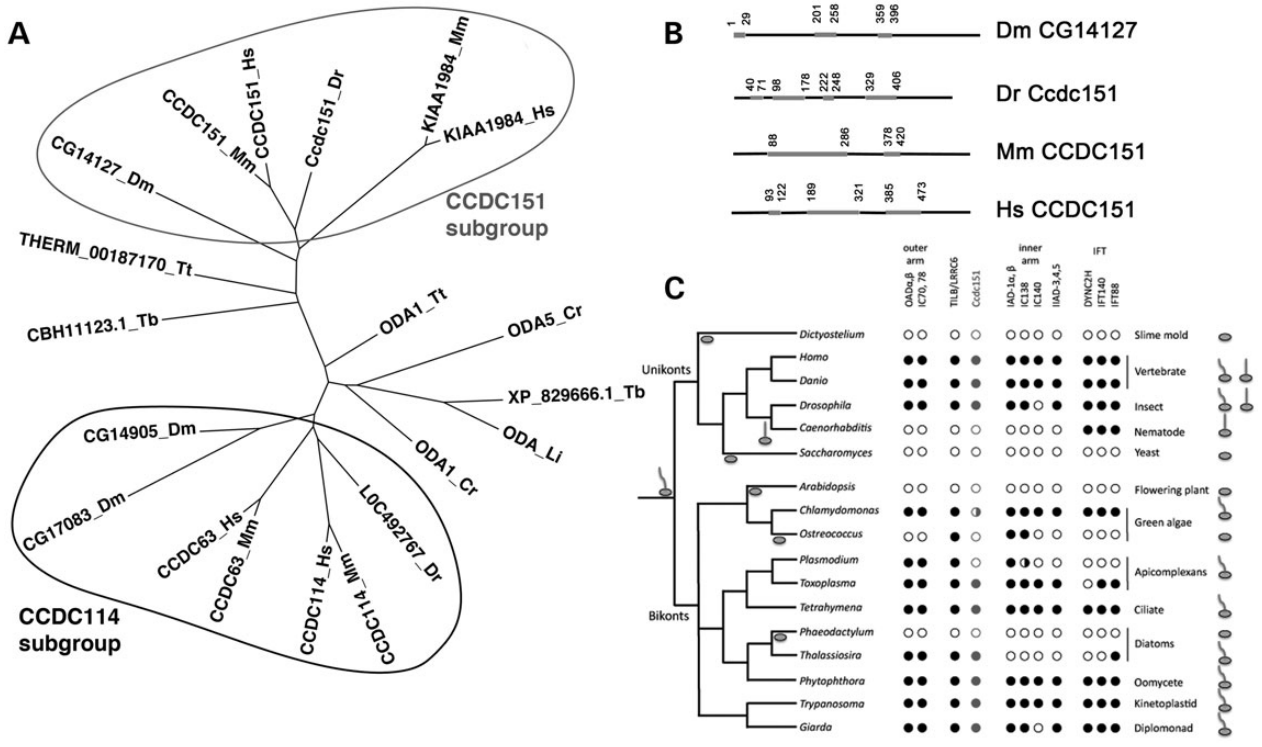

Figure 1. CCDC151 family members share conserved evolutionary features with ODA1. (**A**) Phylogenetic analysis of the proteins related to *Chlamydomonas* ODA1 in *Drosophila*, zebrafish, mouse, humans, *Trypanosoma brucei* and *L. donovani*. Two main branches can be distinguished. The CCDC151 subgroup presents only one ortholog in *Drosophila* (Dm, CG14127, NP_648520) and zebrafish (Dr, CCDC151, NP_001070837) and two paralogs in mice (Mm, CCDC151, NP_084215 and KIAA1984, NP_084135) and humans (Hs, CCDC151, NP_659482 and KIAA1984, NP_001034463). The second subgroup includes several members in animals including two members in *Drosophila* (CG14905, NP_650569 and CG17083, NP_651139), one member in the zebrafish (LOC492767, NP_001007409) and two members in mouse (CCDC63, NP_899130 and CCDC114, NP_001028415) and humans (CCDC63, NP_689804 and CCDC114, NP_653178). Tt, *T. thermophila* (ODA1, XP_001011849); Cr, *Chlamydomonas reinhardtii* (ODA1, XP_001701436; ODA5, AAS10183); Tb, *T. brucei* (XP829666); Li, *L. donovani* (ODA, ACT22628). (**B**) Position of the coiled-coil domains (gray) in *Drosophila*, zebrafish, mouse and human proteins. (**C**) Occurrence of CCDC151 proteins in the eukaryotic kingdom. No CCDC151 orthologs can be found in species with no cilia or non-motile cilia. Reciprocal Best Hits in PSI-Blast run 2 with human CCDC151 as input sequence are noted as gray circles. When no Reciprocal Best Hit was obtained by PSI-Blast run 2, hemi-gray circles were attributed. *Danio rerio*: Ccdc151 (*e*-value = 0); *Drosophila melanogaster*: CG14127 (*e*-value = 2e − 91); *C. reinhardtii*: ODA1 (*e*-value = 6e − 30); *Toxoplasma gondii*: TGME49_082030 (*e*-value = 6e − 77); *T. thermophila*: TTHERM_00187170 (*e*-value = 3e − 69); *Phytophthora infestans*: XP_002898111 (*e*-value = 7e − 82); *T. brucei*: XP_847271 (*e*-value = 2e − 19); *Giardia intestinalis*: GL50581_118 (*e*-value = 1e − 35); *Thalassiosira pseudomona*: XP_002289840 (*e*-value = 6e − 76).

inside the cytoplasm and hence does not rely on IFT (31). All these observations suggest that CCDC151 may play an important function in motile cilia that rely on IFT for their assembly.

CCDC151 is associated with motile IFT-dependent cilia in animals

To address the function of *Ccdc151*, we first characterized its expression profile and subcellular distribution in several model organisms. In mice, *Ccdc151* expression is strongly induced during *in vitro* differentiation of motile cilia of ependymal cells (Fig. 2A). *Ccdc151* expression was down-regulated in ependymal cells obtained from *Rfx3*−/− mice (not shown) (32,33). We designed an antibody directed against the mouse CCDC151 protein (Antibody 1, see Materials and Methods and Supplementary Material, Fig .S2). In mouse ependymal primary cell culture, CCDC151 is associated with motile cilia (Fig. 2B). Identical results were obtained with a commercial antibody directed against the human CCDC151 protein that cross-reacts with the mouse CCDC151 protein (Antibody 2, Supplementary Material, Fig. S2; not shown). Next, we constructed transgenic *Drosophila* expressing a GFP-tagged version of CG14127/CCDC151 under the regulation of its own promoter (see Materials and Methods). In *Drosophila* embryos, we observed CG14127-GFP only in ciliated sensory neurons of the peripheral nervous system (PNS) (Fig. 2C). In addition, GFP expression was restricted to a subset of the ciliated neurons, namely the chordotonal neurons, the only neurons with motile 9 + 0 cilia in *Drosophila* (28,34,35). In these cells, CG14127-GFP was found in the cell body and associated with the ciliary rootlet inside the dendrite and present within the ciliary ending at the tip of the dendrite (Fig. 2C). Importantly, there was no apparent expression of CG14127-GFP in external sensory neurons that have non-motile ciliated endings. Moreover, GFP labeling was absent within motile flagella of spermatozoids. In *Drosophila*, unlike other species, sperm flagellum assembly does not require IFT, whereas sensory cilia do (29,30). Therefore, CG14127/CCDC151 protein expression is restricted to motile cilia that require IFT for their assembly in *Drosophila*.

In zebrafish, we analyzed the expression profile of *ccdc151* during embryonic and larval development. By RT–PCR

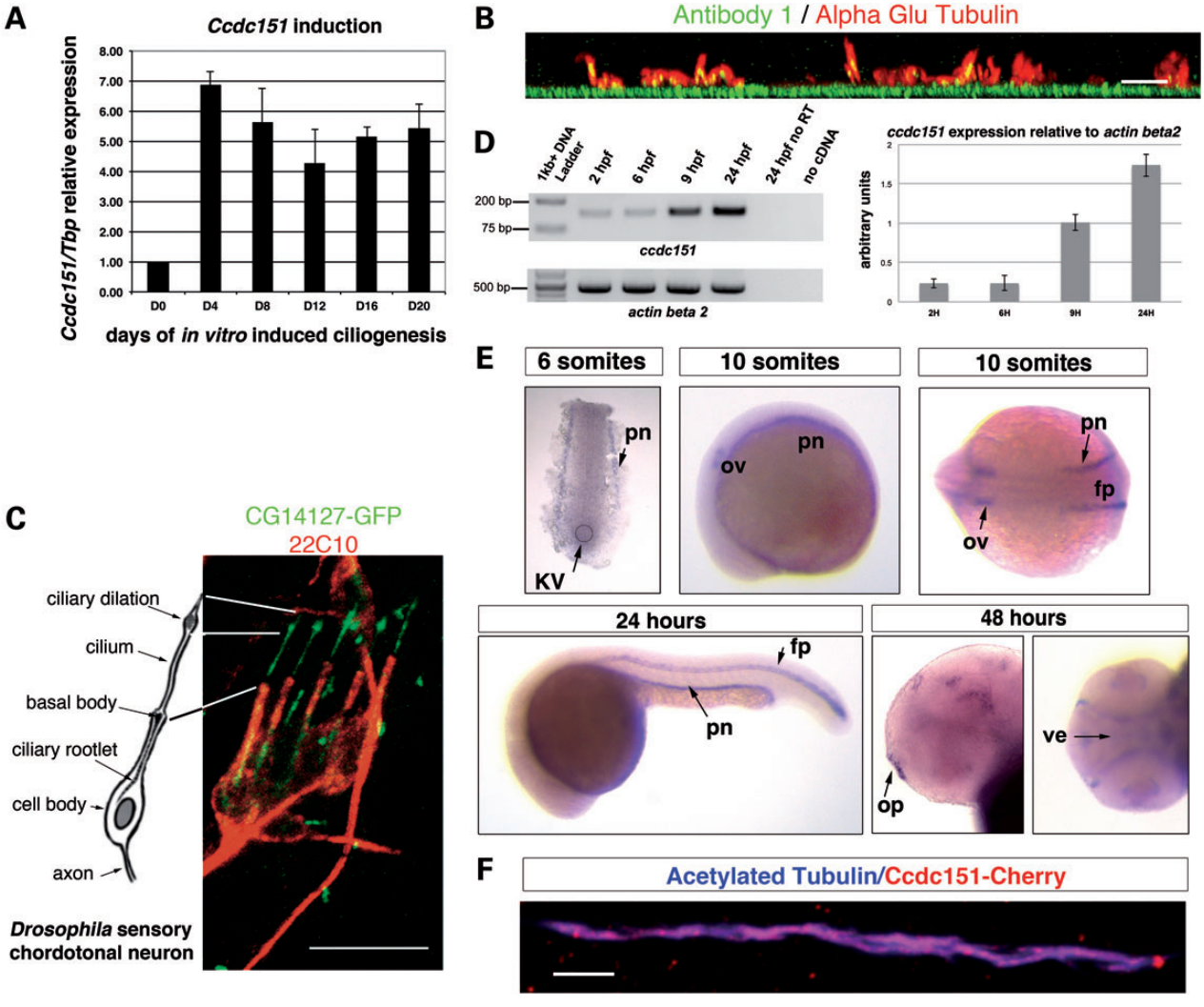

Figure 2. CCDC151 expression is restricted to ciliated cells in animals. (**A**) *Ccdc151* expression is strongly enhanced during *in vitro* ciliogenesis of mouse ependymal cells. Ciliogenesis was induced by serum deprivation at day 0 and *Ccdc151* mRNAs were quantified by real-time RT–PCR and normalized to *Tbp* expression. Results are expressed relative to values at day 0. (**B**) Antibodies directed against mouse CCDC151 protein (Antibody 1) label motile cilia of *in vitro* differentiated mouse ependymal cells as observed on Y projections of confocal images. Cilia are labeled with anti-Alpha Glu Tubulin (red). (**C**) Scheme of an embryonic ciliated neuron of a *Drosophila* chordotonal organ and associated CG14127/CCDC151-GFP expression in transgenic *Drosophila* embryos (stage 17). GFP expression is restricted to the chordotonal organs as observed in the five lateral organs of the larval segments. GFP staining is concentrated in the entire ciliated ending and is also found along the ciliary rootlet inside the dendrite and in the cell body. The PNS (red) is labeled with an anti-Futsch antibody (22C10). (**D**) Maternal and zygotic expression of *ccdc151* in zebrafish. PCR was performed on cDNA from wild-type embryos of 2, 6, 9 and 24 h.p.f. with primers F12 and R13 (left upper panel). Size of the PCR product: 132 bp. Left lower panel: *actin beta 2* control PCR with primers F-actin and R-actin. Right panel: *ccdc151* expression relative to *actin beta 2*. Data are presented as mean ± SD ($n = 3$). (**E**) *In situ* hybridization of zebrafish embryos with *ccdc151* antisense probe. *ccdc151* signal is already detected at six-somite stage in the KV. At 10-somite stage, a strong *ccdc151* expression is observed in the lateral mesoderm corresponding to prospective pronephros territory (pn), the otic vesicle (ov) and the floor plate (fp) as observed on a dorsal view or a lateral view (upper panel). At 24 h, a strong signal is observed in the pronephros (pn) and the floor plate (fp) (lower panel). At 48 h, signal is also observed in the olfactory pit (op) and the cerebral ventricles (ve) (lower panel). (**F**) Immunofluorescence on 24 h.p.f. embryos injected with mRNAs coding for a Cherry-tagged version of Ccdc151 (Ccdc151-Cherry). Ccdc151 is localized in motile cilia of the pronephros. Cilia are labeled with anti-Acetylated Tubulin (blue). Bars: (B) 5 μm; (C and F) 10 μm.

amplification, we first detected *ccdc151* mRNAs as early as 2 h post-fertilization (2 h.p.f.), suggesting a maternal expression of this gene. However, strong expression of *ccdc151* mRNAs started after 6 h.p.f., when zygotic transcription has already been turned on. Levels of *ccdc151* expression increased till 24 h.p.f., the last stage analyzed by this approach (Fig. 2D). By *in situ* hybridization, we first detected *ccdc151* mRNAs in Kupffer's vesicle (KV) (Fig. 2E, upper panel). *ccdc151* mRNAs were later observed in several structures harboring motile cilia, among which are the pronephros (pn), the floor plate (fp) of the neural tube and the otic vesicles (ov) (Fig. 2E, upper panel). Expression in these structures was maintained at later developmental stages, and *ccdc151* mRNAs could also be detected in the olfactory pit (op) and cerebral ventricles (ve), which all present motile cilia (Fig. 2E, lower panel). To examine Ccdc151 subcellular distribution in the zebrafish, we injected *cherry*-tagged *ccdc151* mRNAs. Ccdc151-Cherry was found to be associated with the axoneme of motile cilia in the pronephros (Fig. 2F). Altogether, these results suggest that, like in mice and *Drosophila*, Ccdc151 is associated with motile cilia in zebrafish.

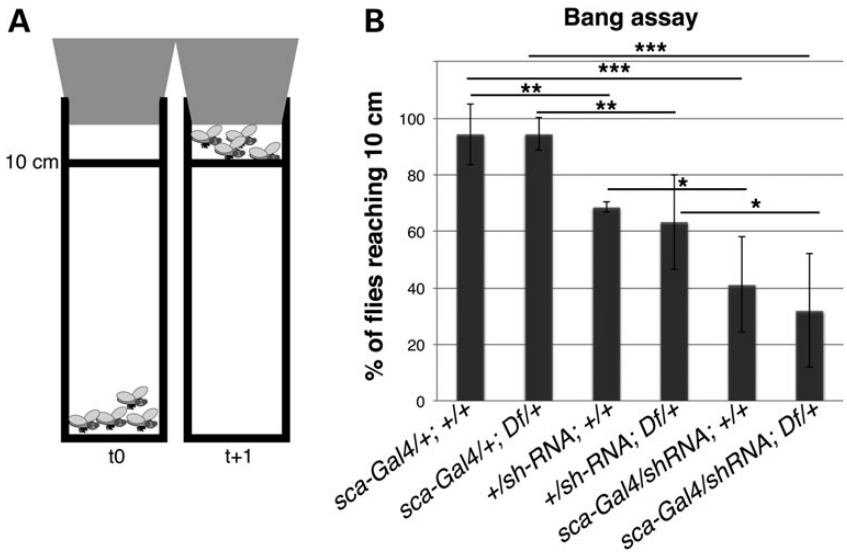

Figure 3. CG14127/CCDC151 depletion in *Drosophila* sensory neurons leads to behavioral defects. (**A**) Scheme of the bang assay used to evaluate fly coordination. (**B**) The percentage of flies that climb >10 cm are scored during 1 min after taping the test tube. Flies carrying *scabrous-Gal4* (*sca-Gal4*) driver and *UAS-shRNA* targeting *CG14127* show a reduced score compared with flies carrying only the *sca-Gal4* driver. No significant differences were observed with the deletion *Df(3L)Exel6115*. All flies carry Dicer-2 on the X chromosome. Two-tailed paired Student's *t*-test analysis was performed to evaluate significant variations. $^{*}P < 0.05$, $^{**}P < 0.01$, $^{***}P < 0.001$.

CG14127/CCDC151-depleted *Drosophila* show defective coordination and geotaxis behaviors

In *Drosophila*, we investigated the function of CG14127 by driving expression of shRNAs in chordotonal neurons of the PNS by using the UAS-GAL4 system. Chordotonal neurons are required for coordinated movement, geotaxis and hearing in *Drosophila* (36,37). Defects in chordotonal neuron function can be assessed by a simple geotaxis behavioral test called bang assay. Flies are tapped to the bottom of a test tube and recorded for 1 min after the bang. The percentage of flies that are able to climb above 10 cm during this first minute is quantified (Fig. 3A). One hundred percent of control flies with the *sca-Gal4* driver only (expressing Gal4 in all PNS neurons) showed negative geotaxis and moved quickly upward in the test tube (Fig. 3B). No significant difference could be observed between these control flies and flies heterozygous for a complete deletion of *CG14127* (*Df(3L)Exel6115*). In contrast, flies harboring an shRNA transgene targeting *CG14127* were less prone to climb on vertical surfaces and the phenotype was significantly more severe in the presence of the *sca-Gal4* driver. The severity of the phenotype in flies heterozygous for a complete deletion of *CG14127* (*Df(3L)Exel6115*) and expressing the shRNA was similar to the one exhibited by flies which only express the shRNA, demonstrating that shRNA silencing was very efficient. These results show that CG14127 is required for proper function of chordotonal neurons in *Drosophila* adults.

Ccdc151-depleted zebrafish show left–right asymmetry defects and kidney cysts

To gain insights into *ccdc151* function in vertebrates, we performed a morpholino (Mo) knockdown approach in zebrafish. We designed two Mos targeted to the translation start site or the second exon-splicing site of the *ccdc151* transcript (exon2–intron2 junction, Supplementary Material, Fig. S3). Both Mos induced similar phenotypes. Rescue experiments with zebrafish full-length *ccdc151* mRNAs, not targeted by the splicing Mo, attest for the specificity of the phenotypes. We therefore present only the results obtained with the splicing Mo. Mo injections led to a characteristic curved-tail phenotype [Fig. 4A, 37% of curved tail in *ccdc151* Mo-injected embryos ($n = 216$), 8% in rescued embryos ($n = 208$) and no curved tail in control embryos, $n = 180$] that is associated with several mutations in genes required for zebrafish cilia assembly or function (38–40). Forty-two percent of Ccdc151-depleted embryos present a reverted cardiac rotation and 24% had no cardiac rotation as visualized by *cmlc2 in situ* hybridization (Fig. 4B), demonstrating that Ccdc151 is required for left–right asymmetry specification. This phenotype was confirmed by aberrant *southpaw* (*spaw*) expression at early stages of left–right embryonic patterning (Fig. 4C). When targeting the Mos specifically into the dorsal forerunner cells (DFC), the precursors of the KV (41–43), we observed an identical phenotype (Fig. 4D), showing that Ccdc151 is required in the KV cells for proper left–right asymmetry specification.

We also observed pronephros dilation and small kidney cysts in 33% of Mo-injected embryos ($n = 216$) that were never seen in control embryos ($n = 180$) (Fig. 4E and F) and rescued by the injection of full-length *ccdc151* mRNAs (11% of embryos with kidney cysts, $n = 208$). However, even the highest doses of injected Mos did not provoke large kidney cysts. We observed hydrocephalus sporadically (1%, Supplementary Material, Fig. S4). We did not observe obvious defects of the otholiths (not shown), nor of the otic kinocilia (Supplementary Material, Fig. S5), even though *ccdc151* mRNAs are present in the otic vesicle (Fig. 2) and that Ccdc151-Cherry can be found in cilia of the otic vesicle (Supplementary Material, Fig. S5).

Altogether, these macroscopic observations show that Ccdc151 plays a critical function in both the KV and the pronephros.

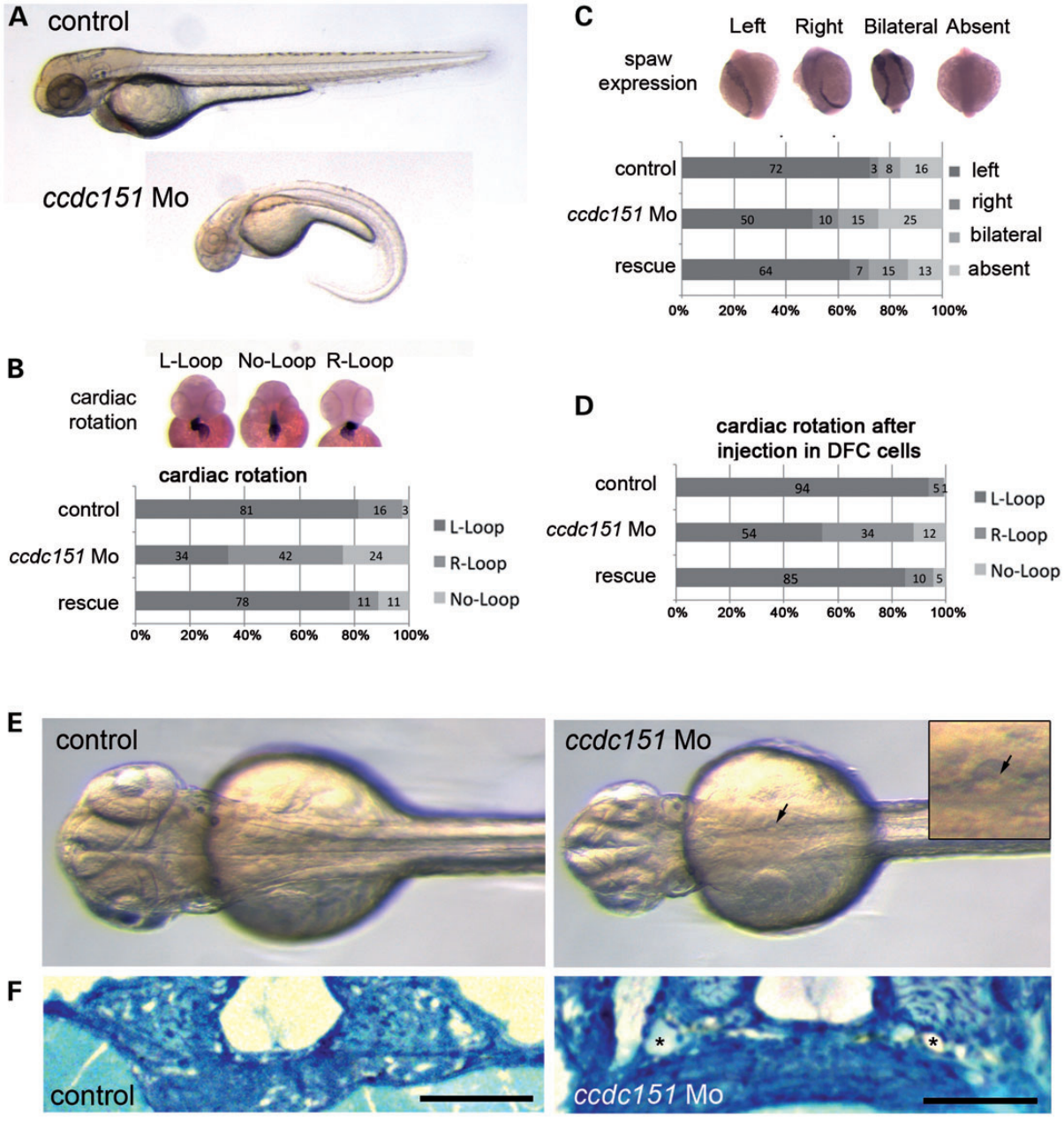

Figure 4. Ccdc151 depletion leads to curved-tail, left–right asymmetry defects and kidney cysts. (**A**) At 48 h.p.f., *ccdc151* morphants exhibit an abnormal ventral axis curvature compared with control embryos. (**B**) *In situ* hybridization of control and *ccdc151* morphants with *cmlc2* probe illustrating the three laterality classes of cardiac loop rotation observed in control or injected embryos. The percentage of each class in control, morphant and rescue embryos is reported on the graph after injection at one-cell stage (four independent experiments, control: $n = 579$, *ccdc151* Mo: $n = 478$, rescue: $n = 216$). (**C**) *In situ* hybridization of control and *ccdc151* morphants showing the four different classes associated with *southpaw* expression in the lateral mesoderm. The percentage of each class in control, morphant and rescue embryos is reported on the graph (three independent experiments, control: $n = 291$, *ccdc151* Mo: $n = 321$, rescue $n = 121$). (**D**) Percentage of the three laterality classes of cardiac loop rotation, observed by *in situ* hybridization with *cmlc2* probe, in control, morphant or rescue embryos after targeting DFC only (four independent experiments, control: $n = 128$, *ccdc151* Mo: $n = 142$, rescue: $n = 254$). (**E**) *ccdc151* morphants exhibit kidney cysts (arrows). Enlarged view of the cyst is presented in the inset. (**F**) Cross-sections of control and *ccdc151* morphant pronephros at 2.5 d.p.f. showing cyst formation (stars). Scale bars: 100 μm

Ccdc151 is required for efficient cilia motility in the zebrafish

To understand the function of Ccdc151, we analyzed the number, distribution and length of cilia in the KV and the pronephros by immunostaining in control and morphant embryos. Cilia length was similar in the presence or in the absence of Ccdc151 (Fig. 5A and C). However, morphants exhibit morphogenesis defects with an enlarged KV with more monociliated cells compared with control embryos (Fig. 5A and B). To assess cilia motility in the KV, we performed live imaging of the fluid flow. Control KV produced an efficient leftward flow, which is visualized by the movement of particles within the vesicle. In contrast, no flow was observed in the morphant KVs and most particles remained immotile (Fig. 5D,

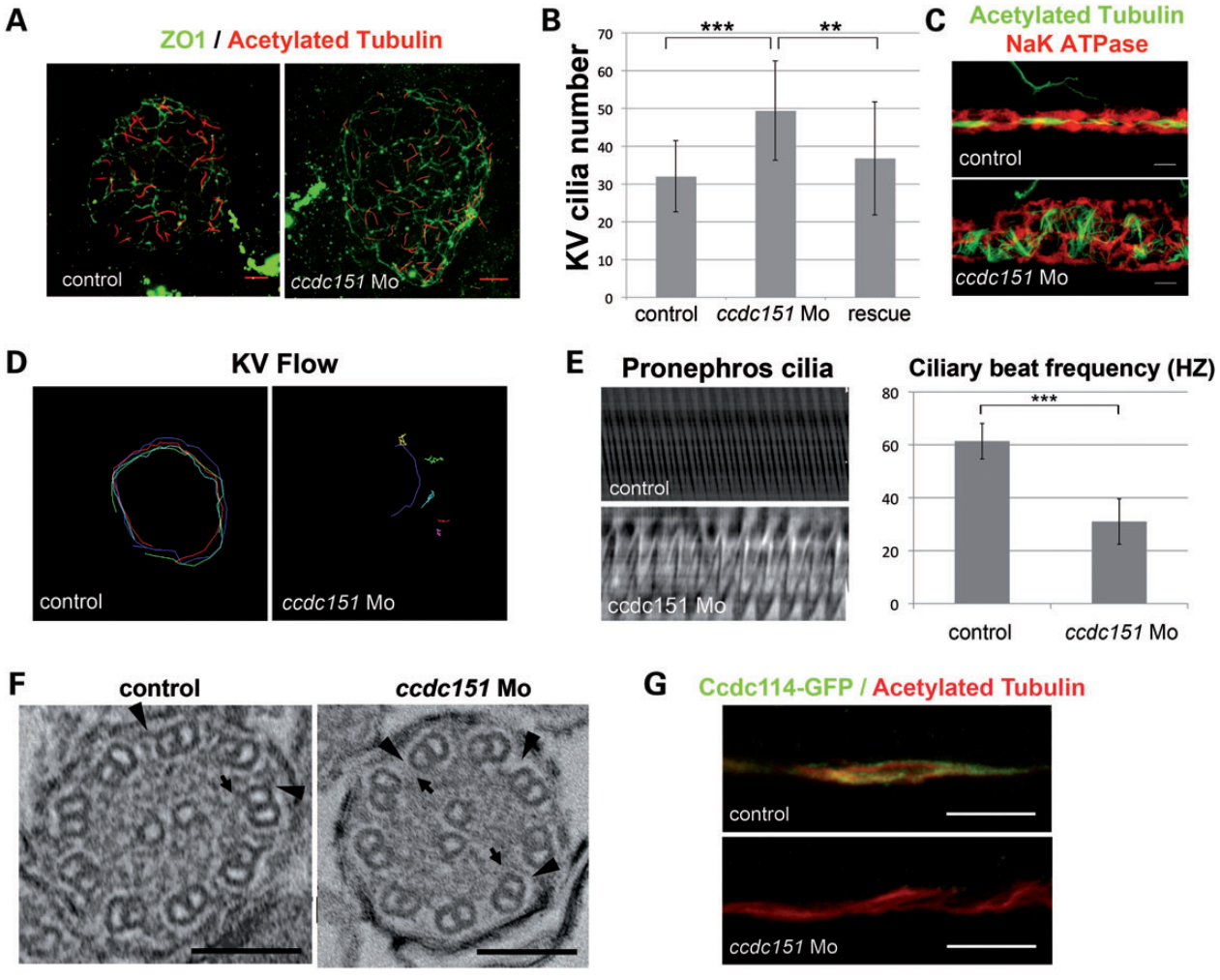

Figure 5. Ccdc151 is required for efficient cilia motility and axonemal dynein assembly on the axoneme. (**A**) 9–10-somite stage *ccdc151* morphants exhibit a larger KV compared with control embryos. Cilia are labeled with anti-Acetylated Tubulin (red) and cell junctions with anti-ZO1 (green). (**B**) The number of ciliated cells is increased but cilia length is not affected in the morphants (two independent experiments, control: $n = 17$, *ccdc151* Mo: $n = 28$, rescue: $n = 14$). (**C**) Immunostaining of the pronephric duct at 48 h.p.f. showing tubule dilation in *ccdc151* morphants compared with control. Cilia are labeled with anti-Acetylated Tubulin (green) and cell membranes with anti-NaK ATPase (red). (**D**) Particle movements were tracked in live control and *ccdc151* morphants at five- to six-somite stages. A counterclockwise circular movement is observed in control KV but no particle movement is observed in the KV of *ccdc151* morphants (control: $n = 6$, *ccdc151* Mo: $n = 7$). (**E**) Line scan analysis of cilia beating movement in control and *ccdc151* morphants at 2.5 d.p.f. The graph indicates the average beating frequency in control and morphants. (**F**) Cross-sections of pronephros motile cilia in control or *ccdc151* morphants. In *ccdc151* morphants, axonemes do not assemble a full complement of IDA and outer dynein arms (arrows and arrowheads) (control: $n = 40$ cilia from 5 embryos, *ccdc151* Mo: $n = 45$ cilia from 9 embryos). (**G**) Ccdc114-GFP (green) localizes in motile cilia of the pronephros in control embryos, whereas in *ccdc151* morphants this localization is lost. Cilia are labeled with anti-Acetylated Tubulin (red). (B and E) Two-tailed paired Student's *t*-test analysis was performed to evaluate significant variations relative to control. $^{*}P < 0.05$, $^{**}P < 0.01$, $^{***}P < 0.001$. Bars: (A, C and G) 10 μm, (F) 100 nm.

Supplementary Material, Movies S1 and S2). We can thus conclude that beating of the cilia is either absent or not efficient. We performed high-speed video recording of pronephros cilia in morphant versus control embryos at later stages and observed a reproducible difference in the beating frequencies of motile cilia (Fig. 5E, Supplementary Material, Movies S3 and S4). Altogether, Ccdc151 is required for efficient motility of cilia in the KV and the pronephros in zebrafish.

Ccdc151 is required for proper assembly of dynein arms in the pronephros

To gain insights into the molecular mechanisms that underlie the motility defects, we analyzed the ultrastructure of pronephric cilia from *ccdc151* morphants. We observed reproducible defects in the number of axonemal dynein arms. This was clearly visualized at the level of the outer dynein arms (Fig. 5F, arrowheads). We also observed a reduced number of IDAs in all embryos analyzed (Fig. 5F, arrows) that was not quantified because of the difficulty to detect IDAs.

Because CG14127/CCDC151 is not a structural component of the *Drosophila* sperm flagella, we hypothesize that it could directly or indirectly be involved in the transport of motile cilia components to the axoneme. We looked for the distribution of Ccdc114, a component of the outer dynein arm-docking complex required for dynein arm attachment onto the axoneme (Fig. 1A) (11,12). We injected *gfp*-tagged *ccdc114* mRNAs in zebrafish together or not with *ccdc151* Mos. Ccdc114-GFP

localized mainly within the axoneme of motile cilia in the pronephros of control embryos. However, in *ccdc151* morphants, the amount of Ccdc114-GFP was strongly reduced (Fig. 5G). Hence, these observations show that Ccdc114 accumulation inside cilia relies on Ccdc151. Altogether, these observations support the requirement of Ccdc151 for targeting dynein arms and the dynein arm-docking complex to the axoneme.

CCDC151 proteins show cellular functions not associated with motile cilia in vertebrates

In zebrafish, *ccdc151* is expressed at stages preceding motile cilia appearance (Fig. 2D). In addition, Ccdc151-Cherry was also found to be associated with basal bodies in zebrafish embryos, as clearly visualized in the floor plate (Fig. 6A).

In agreement with these observations, we detected several phenotypes in *ccdc151* zebrafish morphants that cannot be explained by cilia motility defects. In floor plate cells, where *ccdc151* is strongly expressed, basal bodies were mislocalized in the morphants compared with controls (Fig. 6B and C). In control embryos, basal bodies were found mostly at the posterior side of the cells, whereas in the morphants, basal bodies were sometimes observed in the center or anterior part of the cell (Fig. 6B and C, white arrowheads).

The mislocalization of basal bodies observed in Ccdc151-depleted embryos could reflect either a primary function of Ccdc151 in cell polarity or a secondary cell polarity defect due to improper ciliary beating. However, we also observed altered orientation of cell divisions in the pronephros of *ccdc151* morphants compared with control (Fig. 6D and E). Such cell division orientation defects have been described for PCP components and in particular for *prickle1*, known also to genetically interact with IFT components (44,45). Hence, we investigated whether *ccdc151* could functionally interact with *prickle1* in zebrafish. When co-injecting suboptimal doses of Mos against *prickle1* and *ccdc151*, we indeed observed synergistic effects as shown by the increase in the number of cysts in the pronephros, compared with the absence or weak effects of each individual Mo (Fig. 6F). As we also observed a synergistic interaction on the orientation of cell divisions that cannot solely be explained by combined effect on cilia motility (Fig. 6G), these observations show that *ccdc151* function is not restricted to cilia motility in the zebrafish. Thus, Ccdc151 plays also a role in the acquisition or maintenance of several aspects of cell polarity such as basal body positioning and mitotic spindle orientation.

CCDC151 was also found to be associated with mouse non-motile cilia. In IMCD3 cells serum-starved to induce primary cilia growth, we observed CCDC151 localization in primary cilia (Fig. 7A). In dividing IMCD3 cells, CCDC151 was enriched at the centrioles as observed using two different specific antibodies (Fig. 7B1–2). By methanol fixation, CCDC151 was also observed at basal bodies of serum-starved IMCD3 (Fig. 7B3). We investigated the function of CCDC151 in mouse primary ciliated cells by siRNA transfection. Knockdown of *Ccdc151* using siRNA #1 in IMCD3 cells that efficiently reduced *Ccdc151* expression (Supplementary Material, Fig. S6) leads to the formation of longer primary cilia compared with cells transfected with a control siRNA after 24 h of serum starvation (Fig. 7C and D). The same results were obtained using siRNA #2 (data not shown). Altogether these observations indicate that CCDC151 has a general function in cilia biogenesis in mammalian cells.

DISCUSSION

We have characterized the functions of CCDC151, a target of the RFX ciliogenic transcription factors. Our evolutionary analysis identified CCDC151-encoding gene only in species with IFT-dependent motile cilia. We performed loss-of-function experiments, which demonstrate that CCDC151 is required for the function of motile cilia, as revealed by geotaxis behavioral defects in *Drosophila* adults, on the one hand, and left–right asymmetry defects and kidney cysts in zebrafish embryos, on the other hand. In addition, we show that CCDC151 controls dynein arm assembly and regulates the amount of the dynein arm-docking component CCDC114. Furthermore, several of our observations in zebrafish and in mouse cell culture suggest additional cellular functions for CCDC151. Strikingly, *ccdc151* is required in the pronephros to control the orientation of cell division and interacts with *prickle1* in this process. In mammalian cells, CCDC151 is required for cilia length control.

CCDC151 is a functional component of IFT-dependent motile cilia

The homology between CCDC151 and ODA1 and ODA5 in *Chlamydomonas* suggests a function as a structural component of the outer dynein arm-docking complex (20,23). However, evolutionary comparisons and analysis of its expression in animals show that CCDC151 is likely not a structural component of the axoneme, the dynein arms or dynein docking complexes. Indeed, CCDC151 cannot be considered as the true ortholog of the *Chlamydomonas* proteins because several other proteins related to ODA1 or ODA5 can be found in vertebrates and flies. In particular, in *Drosophila*, the best reciprocal hit of ODA1 or ODA5 is CG14905 and not CG14127/CCDC151. Besides, unlike CG14127/CCDC151, CG14905 is highly expressed in the testis (46), suggesting a structural role in dynein arm assembly in *Drosophila*. This idea is supported by recent studies demonstrating that *Ccdc114* deficiency in humans causes a complete absence of ciliary ODAs resulting in immotile cilia (11,12). CCDC114 and its paralog CCDC63 are found to be, by best reciprocal hit analysis, the true orthologs of ODA1/DC2. One of the two studies in human patients suggests that they play a redundant function in the testis. It is thus tempting to consider that the CG14905/CCDC114 and CCDC63 subgroup of this family of proteins has conserved a motile function as an associated component of the axoneme, whereas CG14127/CCDC151 has evolved toward a function in IFT-dependent transport of motile components of the axoneme. In support of this hypothesis, we found that the localization of Ccdc114 in zebrafish motile pronephric cilia is strongly reduced in *ccdc151* morphants (Fig. 5G), thereby showing that CCDC151 is required for ciliary localization of CCDC114. Moreover, CCDC151 distribution in fly chordotonal neurons is not restricted to the proximal part of the ciliary endings where dynein arms are located (35), but is also found in the ciliary dilation and distal part of the cilia along the ciliary rootlet, like IFT components. It is also interesting to note that several components required for cilia motility that play a

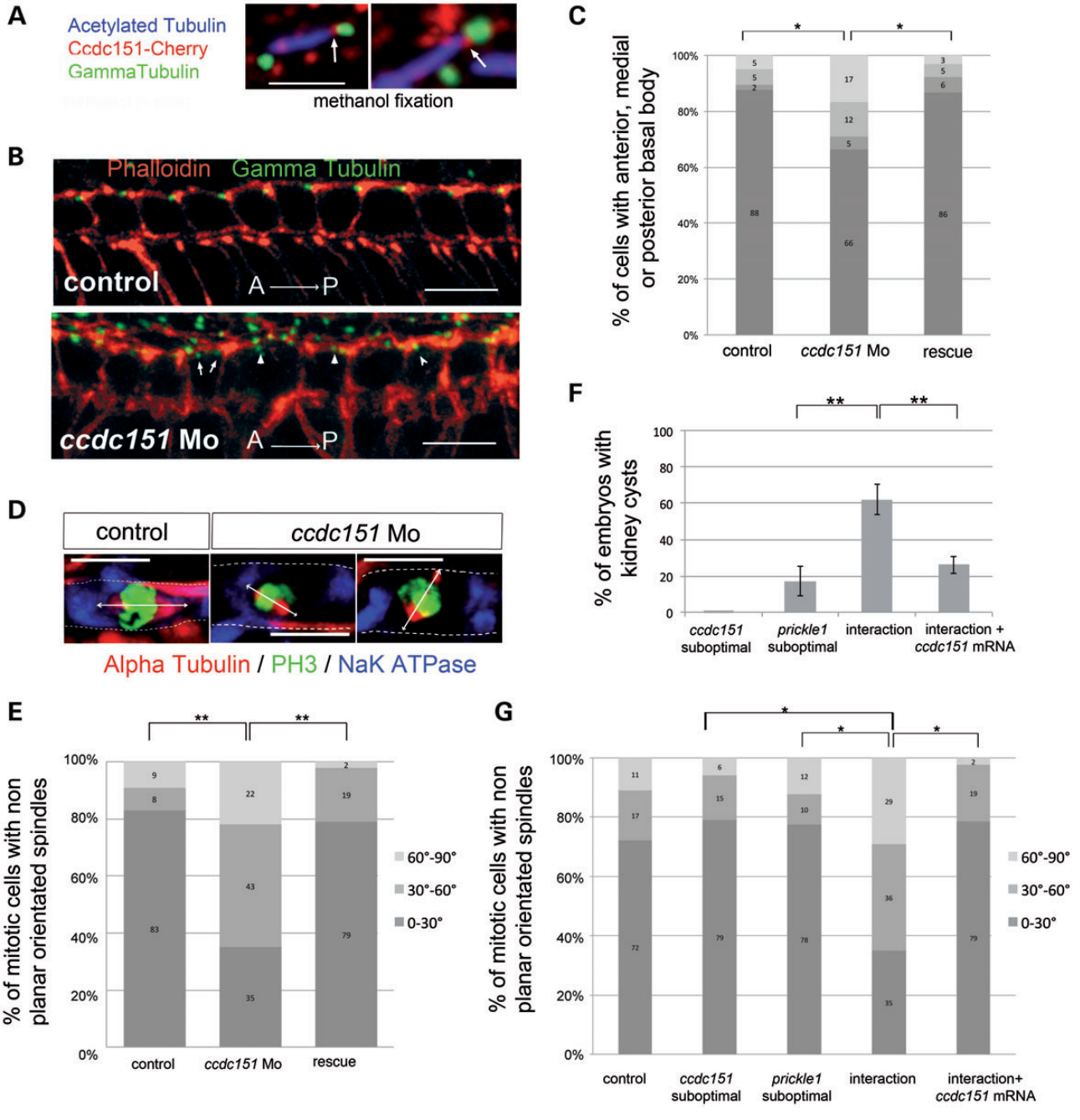

Figure 6. Ccdc151 has cell polarity-associated functions in the zebrafish. (**A**) In 24 h.p.f. zebrafish embryos, Ccdc151 localizes at the basal body of the cilium (arrows, anti-Gamma Tubulin, green) in the floor plate. Cilia are labeled with anti-Acetylated Tubulin (blue). (**B**) Confocal image of 24 h.p.f. control (upper panel) and *ccdc151* morphants (lower panel) showing the basal bodies (green) in floor plate cells. Anterior is to the left. Arrowheads point to some mis-positioned basal bodies in the morphant cells. (**C**) Percentage of floor plate cells with either one basal body in posterior, medial or anterior position (control: $n = 534$ cells in 26 embryos; *ccdc151* Mo: $n = 817$ cells in 37 embryos; rescue: $n = 417$ cells in 20 embryos). The number of mis-positioned basal body is specifically increased in morphant embryos. In a few percentage of cells, more than one Gamma-Tubulin dots that are randomly distributed can be observed (white arrows). These cells are classified as aberrant on the graph. This class is increased in Ccdc151-depleted embryos, which suggest a possible function of the protein in centriole cohesion. (**D**) Lateral confocal image of 48 h.p.f. control and *ccdc151* Mo-injected zebrafish embryos showing mitotic spindles orientation (red) from cells of the pronephric duct. In controls, mitotic spindles are oriented in the longitudinal plane of the duct but not in *ccdc151* morphants. DNA is labeled with anti-PH3 (green). (**E**) The graph indicates the percentage of mitotic cells within three classes of spindle orientations in control, *ccdc151* morphants and rescue from three independent experiments (control: $n = 43$ cells in 30 embryos, *ccdc151* Mo: $n = 63$ cells in 47 embryos, rescue: $n = 31$ cells in 18 embryos). (**F**) The graph illustrates the percentage of kidney cysts after injection of either *ccdc151* or *prickle1* Mos at suboptimal concentrations or after co-injection of the two Mos at suboptimal concentrations [three independent experiments, *ccdc151* Mo suboptimal (no cysts, $n = 57$), *prickle1* Mo suboptimal: $n = 65$, *ccdc151* + *prickle1* suboptimal Mos: $n = 95$, *ccdc151* + *prickle1* suboptimal Mos + *ccdc151* mRNAs $n = 72$]. (**G**) The graph indicates the functional interaction between *ccdc151* and *prickle1* in mitotic spindle orientation (three independent experiments, control: $n = 59$ cells in 21 embryos, *ccdc151* Mo suboptimal: $n = 48$ cells in 22 embryos, *prickle1* Mo suboptimal: $n = 41$ cells in 15 embryos, *ccdc151* + *prickle1* suboptimal Mos: $n = 55$ cells in 29 embryos, *ccdc151* + *prickle1* suboptimal Mos + *ccdc151* mRNAs $n = 31$ cells in 22 embryos). The angles between the spindle axis and the tubule axis were ranked in three classes. When angles are superior to 30°, divisions were considered as non-planar. (E–G) Two-tailed paired Student's *t*-test analysis was performed to evaluate significant variations relative to indicated condition, $^{*}P < 0.05$, $^{**}P < 0.01$, $^{***}P < 0.001$. Bars: (A, B and D) 10 μm.

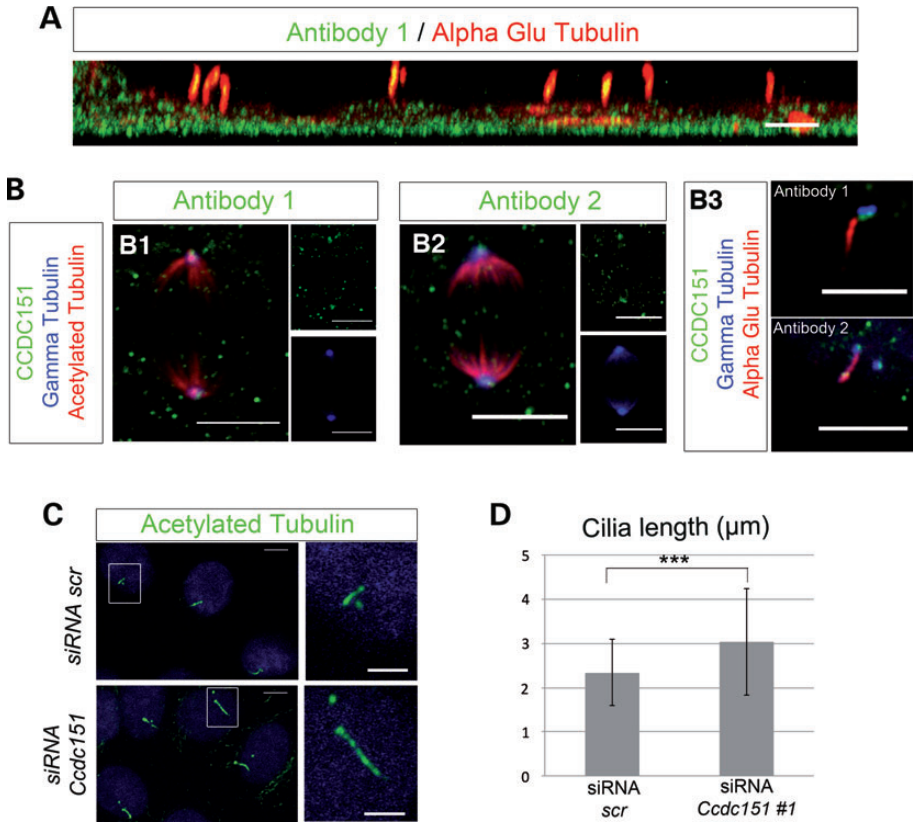

Figure 7. CCDC151 has a non-motile cilia function in IMCD3 cells. (**A**) CCDC151 is present in primary cilia of serum-starved IMCD3 cells fixed in paraformaldehyde solution and stained with two different anti-CCDC151 antibodies (only Antibody 1 is shown). (**B**) CCDC151 is also enriched at centrioles in IMCD3 dividing cells (B1–2), and basal bodies (B3) in serum-starved IMCD3 cells fixed with cold methanol and labeled with either one of the two anti-CCDC151 antibodies. (**C**) Transfection of siRNA directed against *Ccdc151* in IMCD3 cells induces the formation of longer cilia. Enlarged views of selected cilia are presented in insets. Cilia were stained for Acetylated Tubulin (green). (**D**) The graph indicates the mean ciliary length observed in *siRNA scr* and *siRNA Ccdc151 #1* (two experiments, *siRNA scr* $n = 54$ cilia, *siRNA Ccdc151 #1* $n = 56$ cilia). Two-tailed paired Student's *t*-test analysis was performed to evaluate significant variations relative to indicated condition, $^{*}P < 0.05$, $^{**}P < 0.01$, $^{***}P < 0.001$. Scale bars: (A–C) 5 µm (C enlarged insets) 2.5 µm.

structural function at the level of the axoneme and that are conserved in *Drosophila* are expressed in the testis, whereas proteins required for IFT-associated transport of motile components of the dynein arms are not. For example, dynein arm components and DRC proteins (gas8, CG14271; FlyBase) are expressed in the testis, whereas IFT46/CG15161 or WDR69/CG7568 are not [(17,18), FlyBase]. Furthermore, no CCDC151 protein is found in *P. falciparum*, whose motile flagella are assembled in an IFT-independent mode (31). Last, no CCDC151 ortholog is found in the microalgae *Ostreococcus* that have no flagella and no IFT but have retained some IDA components, suggesting that CCDC151 is not required for dynein function *per se*. However, we cannot exclude that CCDC151 has evolved differently in each animal species where it may play very different functions.

Relationships between CCDC151 and other components of the axonemal dynein assembly pathway

Our work suggests that CCDC151 is a novel factor involved in both IDA and outer dynein arm assembly. Several proteins are required for axonemal dynein assembly in different organisms. However, it is not clear how these proteins work together and what are their hierarchical relationships. None of the characterized genes involved in the dynein assembly pathway share functional or evolutionary features with CCDC151. For instance, we show that CCDC151 is associated with motile cilia that require only IFT for their assembly. *Drosophila* is particularly helpful to discriminate between both types of motile cilia, as chordotonal neurons have IFT-dependent motile cilia (35), whereas sperm flagella assembly is IFT independent (29,30). Among the proteins that play a role both in the outer dynein arm and IDA assembly in vertebrates, all show unique orthologs in *Drosophila*, which are strongly expressed in the testis, suggesting an IFT-independent function for these genes. Therefore, DNAAF1/ODA7/LRRC50, DNAAF2/KTU/PF13, CCDC103 and LRRC6, which are required for both IDA and outer dynein arm assembly in humans or fish (6,7,14,15,40,47–49), have unique orthologs in *Drosophila* (*CG1553/Nop17l*, *CG31623*, *CG13202* and *TilB*, respectively) that are strongly expressed in the testis (FlyBase). Like the human ortholog, *TilB/LRRC6* is required for the outer and inner axonemal dynein arm assembly in *Drosophila* sensory cilia and is also required for spermatozoid flagella motility in *Drosophila* (35).

Among the other proteins that have been shown to play a more specific role in either IDA or outer dynein arm assembly, none appear to be restricted to IFT-dependent cilia because their *Drosophila* orthologs are also strongly expressed in the *Drosophila*

testis, unlike CCDC151. This is true for DNAAF3, CCDC39, CCDC40 and CCDC114 (8,9,11,12), whose unique orthologs in *Drosophila* (*DNAAF3/CG17669*, *CCDC39/CG17387* and *CCDC40/CG41265*, *CCDC114/*CG14905) are also strongly expressed in the testis.

Therefore, the only yet described component to be involved in dynein arm assembly and that is apparently not expressed in the *Drosophila* testis is ODA16/WDR69, which is required for IFT-dependent transport of axonemal dyneins from *Chlamydomonas* to zebrafish (16,23,50). These observations show that CCDC151 has evolved like IFT-associated proteins but not like other proteins described to be required for dynein assembly in animals. Hence, these observations reinforce the hypothesis that CCDC151 plays an IFT-associated function required for dynein arm assembly that is different from the function of the other proteins that have been described to date.

In vertebrates, CCDC151 proteins present cellular functions not associated with motile cilia

Our study strongly suggests that CCDC151 proteins have functions in vertebrates that are not restricted to dynein arm assembly. Indeed, in IMCD3 mouse cell cultures, CCDC151 is associated with primary cilia and basal bodies but also with the spindle poles. Knockdown experiments using siRNA against *Ccdc151* lead to the formation of longer cilia. Furthermore, in zebrafish, depletion of Ccdc151 leads to cell division orientation defects in the pronephros. *ccdc151* functionally interacts with *prickle1* in this orientation of cell divisions, suggesting that *ccdc151* plays roles that are not directly related to dynein arm assembly. In *Leishmania donovani*, the sole CCDC151 family member is involved not only in the control of flagellar motility but also in the control of flagellar length (51). This is coherent with our observation that CCDC151 is required for primary cilia length control in IMCD3 cells. Altogether, CCDC151 is associated with processes that are not only linked to cilia motility but related to more general functions in cilia assembly or cell processes such as orientation of cell divisions, which have also been shown to be controlled by IFT proteins (45,52). Based on these observations, we hypothesize that CCDC151 could behave as a bridge, linking IFT proteins to specific cargoes such as dynein arms but also to other cargoes that are required during cell division or in cilia assembly. Such complex interactions between IFT proteins, specific cargoes and, for example, transition zone-associated proteins or dynein arm components have already been described (18,53,54).

In conclusion, our work identifies CCDC151 as a novel protein required for the assembly of motile cilia in vertebrates. *CCDC151* represents a novel candidate gene in which mutations could lead to PCD. Because *ccdc151* also interacts with *prickle1* during cell division, it could also be involved in other primary cilia-associated syndromes where impaired PCP has been implicated in some of the physio-pathological outcomes.

MATERIALS AND METHODS

Zebrafish maintenance

General maintenance, collection and staging of zebrafish were carried out at the PRECI zebrafish facility of IFR 128, Biosciences-Gerland (Lyon, France). The developmental stages are given in hour post-fertilization (h.p.f.) and day post-fertilization (d.p.f.) according to morphological criteria. For somite-stage embryos, the number of somites was used (55). Embryos were kept at 28.5°C in 1× Danieau solution (58 mM NaCl, 0.7 mM KCl, 0.4 mM $MgSO_4$, 0.6 mM $Ca(NO_3)_2$, 5 mM Hepes, pH 7.6) in compliance with French Government guidelines. If necessary, 1-phenyl-2-thiourea (Sigma) was added in medium to avoid pigmentation.

Drosophila stocks

Flies were cultured in standard condition at 25°C. The following fly strain was constructed in the laboratory: *w*, *P{CG14127::GFP}^{M5}*, the transgene was inserted on the X chromosome. *w1118;Df(3L)Exel6115*, *P{XP-U}Exel6115/TM6B*, *Tb1* were obtained from the Bloomington Stock Center. ShRNA expressing strain targeting CG14127 (KK106258) was obtained from the Vienna Drosophila RNAi Center.

Bang assay

The climbing test was performed on 3–5-day-old male flies at identical time point each day. Ten flies were placed in a graduated vial and banged on the table at $t = 0$. Flies were recorded for 1 min after the bang. The movies were analyzed using QuickTime Player (Apple). Each fly climbing >10 cm was scored as positive. Three different batches of 10 flies were analyzed for each genotype. Each batch was successively tested five times and the results were averaged.

Plasmid constructs

All primers are described in Supplementary Material, Table S1.

Drosophila *CG14127* reporter construct
A pJT12 reporter vector was constructed as follows. P5′ from pW8 was inserted within the NaeI and KpnI site of pBSK. A cassette containing both an EGFP-Flag coding sequence (from pEGFP-Flag, kindly provided by S. Treves) and P3′ from pW8 was then inserted in the previous construct within the ClaI (Blunt Ended) and KpnI sites. A 2668 bp fragment including *CG14127* coding sequence and upstream regulatory sequence was amplified by PCR on wild-type *Drosophila* genomic DNA using CG14127-pro5/KpnI and CG14127-pro3/NheI primers. The resulting PCR fragment was cloned into the KpnI and NheI sites of the pJT12 plasmid. The transgenic strain was obtained by P-element-mediated insertion.

pCS2-Ccdc151
The complete zebrafish *ccdc151* coding sequence was obtained by RT–PCR with F1 and R2 primers. The resulting PCR product was cloned into the EcoRI and XbaI sites of the pCS2+ vector. The *ccdc151* sequence was verified by sequencing.

Ccdc151-cherry
The complete zebrafish *ccdc151* coding sequence was obtained by PCR on pCS2-Ccdc151 with F1 and R3 primers. The resulting PCR product was cloned into the EcoRI and AgeI sites of the pCS-mCherry vector in frame with the *cherry* sequence (a gift

from Dr S. Megason). The *ccdc151* sequence was verified by sequencing.

pBSK-Ccdc151
For *in situ* experiments, the first 871 bp of the zebrafish *ccdc151* coding sequence were amplified with F4 and R5 primers. The PCR product was cloned into the EcoRI and XbaI sites of pBSK.

Ccdc114-GFP
The complete zebrafish *ccdc114* coding sequence was obtained by RT–PCR with F8 and R9 primers. The resulting PCR product was cloned into the Spe1 and SnaBI sites of the pCS2+ GFP vector in frame with the *gfp* sequence (a gift from Dr B. Ciruna). The *ccdc114* sequence was verified by sequencing.

mCCDC151-GFP
The complete mouse *Ccdc151* coding sequence was obtained by RT–PCR with F10 and R11 primers. The resulting PCR product was cloned into the HindIII and BamH1 sites of pEGFP-N1 (Clontech) in frame with the *gfp* sequence. The *Ccdc151* sequence was verified by sequencing.

mCCDC151-MYC
The 6xMyc Tag cassette of 263 bp was obtained after PvuI and EcoRI digestion of pCS2+ nlsMT (a gift from Dr R. Rupp). The blunt-ended fragment was cloned in replacement of the GFP cassette from pEGFP-N1 to produce pJTm13. The mouse *Ccdc151* coding sequence was obtained after HindIII and BamHI digestion of the mCCDC151-GFP vector and cloned in the same restriction sites of pJTm13 in frame with the 6xMyc Tag cassette.

RT–PCR analysis

Total RNA of zebrafish embryos was extracted using the Nucleospin Extract II Kit (Macherey-Nagel). cDNA was obtained using 1 or 0.5 μg of DNAse-treated RNA, 200 ng of random primers (Promega) and 200 U of RevertAid H minus M-MuLV reverse transcription (Thermo Fisher Scientific) in a final volume of 40 or 50 μl. Two or 4 μl of cDNA was used for PCR reactions. Primers F12 and R13 were used for *ccdc151* amplification and primers F-actin and R-actin for *actin beta 2* amplification. PCR analyses on three independent RT were performed and quantifications were done using the Molecular Imager GelDoc XR system and the Quantity One software (Bio-Rad).

Real-time RT–PCR

Real-time RT–PCR was performed as described previously (33). The expression of *Ccdc151* (F-mCcdc and R-mCcdc primers) was normalized using the housekeeping gene *Tbp* (TATA binding protein) (56) (F-TBP and R-TBP primers).

Mos and mRNA injection

Mos against *ccdc151* were designed to target either the translation site of the mRNA (AUG) or the splice-donor site of the second coding exon and obtained from GENE TOOLS, LLC, Philomath. The following Mos were used: Mo-ccdc151AUG 5′-AGACCGACGTGCCGGGCATTATATA-3′ and Mo-ccdc 151Ex 5′-AAGATTCATAATGTCTGACCTCAGC-3′. The molecular defect caused by Mo-ccdc151Ex was verified by RT–PCR with primers F6 and R7 located in exons 1 and exon 3, respectively (Supplementary Material, Fig. S3). For functional interaction studies, we used previously described Mos targeting *prickle1* (57). For rescue experiments, the pCS2-Ccdc151 plasmid was linearized and capped mRNAs were transcribed from this template using the mMessage Machine Kit (Ambion).

Mos and purified mRNAs were diluted in 1× Danieau solution containing 0.1% phenol red (Sigma). Four nanograms of Mo-ccdc151Ex were injected at one-cell-stage embryos in a total volume of 500 pl using a micro-injector. For rescue experiments, 4 ng of Mo-ccdc151Ex and 80 pg of zebrafish *ccdc151* mRNAs were co-injected. For functional interaction, 3 ng of Mo-ccdc151Ex and 0.65 ng of Mo-prickle1 were co-injected. For DFC injections, fluorescein-labeled Mo-ccdc151Ex was injected into the yolk of 512-cell-stage embryos as previously described (58). For localization, 20 pg of *ccdc151-cherry* and 20 pg *of ccdc114-gfp* ± 4 ng of Mo-ccdc151Ex were injected.

Antibodies

The following primary antibodies and dilutions were used: Acetylated Tubulin 6-11B-1 (Sigma, 1/500), NaK/ATPase α6F (DSHB, 1/500), Gamma Tubulin GTU88 (Sigma, 1/1000), phalloidin rhodamin (Interchim, 1/200), ZO1 (Zymed, 1/25), Alpha Tubulin (Sigma, 1 /500), Phosphohistone H3 (Santa cruz, 1/750), Dsred living colors (Clonetech, 1/500), Alpha Glu Tubulin (1D5-Synaptic systems, 1/100), GFP (Molecular Probes, 1/500), anti-Futch 22C10 (a gift from Dr S. Benzer, 1/500), Human CCDC151 (Abnova 1/200). Secondary antibodies were from Molecular Probes/Invitrogen™/ Life Technologies for immunofuorescence analysis. For western blot analysis, the following antibodies were used: goat anti-guinea pig-HRP (Jackson 1/10 000), goat anti-rabbit-HRP and goat anti-mouse-HRP (Bio-Rad, 1/3000).

Generation of antibodies against mouse CCDC151

The first 300 bp of the mouse *Ccdc151* coding sequence were amplified and cloned in frame with the 6xHis tag in the pSTABY-1 expression vector (Delphi Genetics). The production of the 6xHis tagged protein was performed according to the manufacturer's protocol (Delphi Genetics) and purified using Protino Ni-TED/IDA Combi sample (Macherey-Nagel). Immunization of guinea pigs with the purified protein was performed by Eurogentec.

Immunoblotting

Whole-cell extracts were prepared from COS7 cells that have been transiently transfected with mCCDC151-GFP or mCC DC151-MYC plasmids. Proteins were analyzed by SDS–PAGE and immunoblot analysis according to standard protocols with Antibody 1 (1/200), Antibody 2 (1/200, Sigma) and anti-GFP (1/1000, Roche). Appropriate HRP-conjugated secondary antibodies were used for detection by chemiluminescence using the Immun-Star WesternC Kit from Bio-Rad.

Whole-mount *in situ* hybridization

Whole-mount *in situ* hybridizations were carried out as described previously (59). RNA probes were synthetized using a Digoxigenin RNA Labeling Kit (Roche) according to the manufacturer's instruction. A sense RNA probe complementary to the specific zebrafish *ccdc151* probe was prepared as negative control. The stained embryos were fixed and photographed with a Leica 425C camera.

Cell culture

Mouse primary ependymal cell cultures were derived from mouse newborn brains (OF1 strain), as previously described (33). IMCD3 cells (a gift from A. Benmerah, Institut Cochin, Paris, France) were cultured in DMEM/HAM'S F12 medium containing 10% FBS, 100 U/ml penicillin, 100 μg/ml streptomycin and 1× non-essential amino acids. COS7 cells were cultured in DMEM medium containing 10% FBS, 100 U/ml penicillin, 100 μg/ml streptomycin (reagents from GE Healthcare).

Transfection and siRNA

For plasmid transfection, cells at 80–90% confluency were transfected with Lipofectamine 2000 according to the manufacturer's instructions. For RNAi knockdown, individual siRNA from Sigma (siRNA *Ccdc151* #1) and siGENOME SMARTpool siRNA containing four different duplexes from Dharmacon (siRNA *Ccdc151* #2) were designed against mouse *Ccdc151* sequence using their custom services. Antisense sequences were as follows:

siRNA *Ccdc151* #1: 5′-ACUACCAGCAGAUUGUAAG-3′;
siRNA *Ccdc151* #2: 5′-UCCAUUGGGAGCUCUCAUA, 5′-UAAUGCUCGCUUCUUGC-3′, 5′-AUCAUUGUGACG CUGCUCC-3′, 5′-UAAGCGUAGUCCUCUGAGU-3′.

siGENOME Non-Targeting siRNA #2 (Dharmacon) was used as a negative control. For immunofluorescence experiments, 40 000 IMCD3 cells in 24 wells plate were transfected twice with each siRNA at J0 with 25 pmol and at J2 with 37.5 pmol using Lipofectamine 2000. Cells were serum-deprived 24 h before analysis at 96 h. For real-time RT–PCR analysis, 60 000 IMCD3 cells in 12 wells plate were transfected twice with each siRNA at J0 with 50 pmol and at J2 with 50 pmol using Lipofectamine 2000. RNA was extracted after 24 h serum deprivation at 96 h.

Immunohistochemistry

For immunostaining analysis, staged *Drosophila* embryos were treated as described previously (60).

Cells for immunofluorescence microscopy were grown, fixed and stained as described previously (33). Early zebrafish embryos (before 24 h.p.f.) were fixed 4 h in PFA 4%, washed in PBS 1× –0.3% Triton X-100 and blocked 1 h at room temperature in blocking buffer (1% BSA, 1% DMSO, 2% NGS, 0.3% Triton X-100, PBS 1×, pH7.4). Primary antibodies were incubated in blocking buffer overnight at 4°C. After washes in PBS 1× –0.3% Triton X-100, embryos were incubated with secondary antibodies in blocking buffer for 2 h at room temperature. Embryos at 48 h.p.f. were fixed in Dent's buffer (80% methanol/20% DMSO) overnight at 4°C (or 4 h at RT for GFP labeling) and stained as described in Kramer-Zucker *et al*. (38).

Histology

Zebrafish embryos were fixed overnight in 4% PFA before preparation for histology according to Sullivan-Brown *et al*. (61). The embedded embryos were sectioned at 4 μm with a Leica RM2265 microtome. The sections were stained with azur/methylene blue (1/1). Slides were examined using an Axio Imager Z1 (Zeiss) microscope.

Electron microscopy

Whole embryos were fixed in a mixture of 1.5% glutaraldehyde and 1% paraformalaldehyde in 0.2 M cacodylate buffer (pH 7.4) for 3 h at room temperature. The samples were postfixed for 0.75 h in 1% OsO4 in 0.15 M cacodylate buffer. The samples were then rinsed in 0.15 M cacodylate buffer, dehydrated in a graded series of ethanol, embedded in Epon 812 (Fluka) and 1 μm sections observed after toluidine blue staining. Ultra-thin sections were contrasted with uranyl acetate and lead citrate and examined with a Philips CM 120 electron microscope.

Fluid flow recording in the KV

At four- to five-somite stages, embryos were mounted with the KV positioned upright in 1% low-melting agarose. The rotating particles were imaged using a spectral SP5 microscope (Leica) with a 40× water immersion lens. All movies were slowed down to 25 frames per second (f.p.s.).

High-speed video microscopy

Live embryos were incubated in drops of 1% low-melting agarose containing 0.4% tricaine (Sigma) and oriented along their lateral sides. Cilia motility was recorded with a Leica DM-RXA microscope equipped with a 60× water immersion objective and differential interference contrast optics. Videos were recorded with a PCO 1200 high-speed camera at 500 f.p.s. All movies were slowed down to 25 f.p.s.

SUPPLEMENTARY MATERIAL

Supplementary Material is available at *HMG* online.

ACKNOWLEDGEMENTS

We thank Jérôme Schmitt and Patricia Morales for *Drosophila* medium and stock maintenance and Laure Bernard and Bernard Perret for zebrafish maintenance. Electron microscopy was performed at the Centre Technologique des Microstructures of the University of Lyon (CTmu) with the help of Jean-Luc Duteyrat. We are grateful to Yves Tourneur and Denis Ressnikoff from the Centre Commun de Quantimétrie of the University of Lyon and to Christophe Chamot from the Platim at the ENS-Lyon for their help in imaging. We also thank Laurent Duret for help with the phylogenetic analysis and Sylvie Schneider Maunoury for helpful discussions.

Conflict of Interest statement. None declared.

FUNDING

This work was supported by grants to B.D. from the Fondation pour la Recherche Médicale (équipe FRM 2009), the ANR (Ciliopath-X) and the Région Rhône-Alpes (Cible 2008). F.S. was supported by a doctoral fellowship from the Région Rhône-Alpes. J.J. was supported by a Fondation Line Pomaret Delalande award. B.C. was supported by a postdoctoral fellowship from the Fondation pour la Recherche Médicale.

REFERENCES

1. Nigg, E.A. and Raff, J.W. (2009) Centrioles, centrosomes, and cilia in health and disease. *Cell*, **139**, 663–678.
2. Bettencourt-Dias, M., Hildebrandt, F., Pellman, D., Woods, G. and Godinho, S.A. (2011) Centrosomes and cilia in human disease. *Trends Genet.*, **27**, 307–315.
3. Leigh, M.W., Pittman, J.E., Carson, J.L., Ferkol, T.W., Dell, S.D., Davis, S.D., Knowles, M.R. and Zariwala, M.A. (2009) Clinical and genetic aspects of primary ciliary dyskinesia/Kartagener syndrome. *Genet. Med.*, **11**, 473–487.
4. Huang, B., Piperno, G. and Luck, D.J. (1979) Paralyzed flagella mutants of *Chlamydomonas reinhardtii*. Defective for axonemal doublet microtubule arms. *J. Biol. Chem.*, **254**, 3091–3099.
5. Kobayashi, D. and Takeda, H. (2012) Ciliary motility: the components and cytoplasmic preassembly mechanisms of the axonemal dyneins. *Differentiation*, **83**, S23–S29.
6. Panizzi, J.R., Becker-Heck, A., Castleman, V.H., Al-Mutairi, D.A., Liu, Y., Loges, N.T., Pathak, N., Austin-Tse, C., Sheridan, E., Schmidts, M. *et al.* (2012) CCDC103 mutations cause primary ciliary dyskinesia by disrupting assembly of ciliary dynein arms. *Nat. Genet.*, **44**, 714–719.
7. Loges, N.T., Olbrich, H., Becker-Heck, A., Häffner, K., Heer, A., Reinhard, C., Schmidts, M., Kispert, A., Zariwala, M.A., Leigh, M.W. *et al.* (2009) Deletions and point mutations of LRRC50 cause primary ciliary dyskinesia due to dynein arm defects. *Am. J. Hum. Genet.*, **85**, 883–889.
8. Merveille, A.-C., Davis, E.E., Becker-Heck, A., Legendre, M., Amirav, I., Bataille, G., Belmont, J., Beydon, N., Billen, F., Clément, A. *et al.* (2011) CCDC39 is required for assembly of inner dynein arms and the dynein regulatory complex and for normal ciliary motility in humans and dogs. *Nat. Genet.*, **43**, 72–78.
9. Becker-Heck, A., Zohn, I.E., Okabe, N., Pollock, A., Lenhart, K.B., Sullivan-Brown, J., McSheene, J., Loges, N.T., Olbrich, H., Haeffner, K. *et al.* (2011) The coiled-coil domain containing protein CCDC40 is essential for motile cilia function and left-right axis formation. *Nat. Genet.*, **43**, 79–84.
10. Mitchison, H.M., Schmidts, M., Loges, N.T., Freshour, J., Dritsoula, A., Hirst, R.A., O'Callaghan, C., Blau, H., Al Dabbagh, M., Olbrich, H. *et al.*. (2012) Mutations in axonemal dynein assembly factor DNAAF3 cause primary ciliary dyskinesia. *Nat. Genet.*, **44**, 381–389, S1–S2.
11. Onoufriadis, A., Paff, T., Antony, D., Shoemark, A., Micha, D., Kuyt, B., Schmidts, M., Petridi, S., Dankert-Roelse, J.E., Haarman, E.G. *et al.* (2012) Splice-site mutations in the axonemal outer dynein arm docking complex gene CCDC114 cause primary ciliary dyskinesia. *Am. J. Hum. Genet.*, **92**, 88–98. .
12. Knowles, M.R., Leigh, M.W., Ostrowski, L.E., Huang, L., Carson, J.L., Hazucha, M.J., Yin, W., Berg, J.S., Davis, S.D., Dell, S.D. *et al.* (2013) Exome sequencing identifies mutations in CCDC114 as a cause of primary ciliary dyskinesia. *Am. J. Hum. Genet.*, **92**, 99–106.
13. Lee, L. (2011) Mechanisms of mammalian ciliary motility: insights from primary ciliary dyskinesia genetics. *Gene*, **473**, 57–66.
14. Duquesnoy, P., Escudier, E., Vincensini, L., Freshour, J., Bridoux, A.-M., Coste, A., Deschildre, A., de Blic, J., Legendre, M., Montantin, G. *et al.* (2009) Loss-of-function mutations in the human ortholog of *Chlamydomonas reinhardtii* ODA7 disrupt dynein arm assembly and cause primary ciliary dyskinesia. *Am. J. Hum. Genet.*, **85**, 890–896.
15. Omran, H., Kobayashi, D., Olbrich, H., Tsukahara, T., Loges, N.T., Hagiwara, H., Zhang, Q., Leblond, G., O'Toole, E., Hara, C. *et al.* (2008) Ktu/PF13 is required for cytoplasmic pre-assembly of axonemal dyneins. *Nature*, **456**, 611–616.
16. Ahmed, N.T., Gao, C., Lucker, B.F., Cole, D.G. and Mitchell, D.R. (2008) ODA16 aids axonemal outer row dynein assembly through an interaction with the intraflagellar transport machinery. *J. Cell Biol.*, **183**, 313–322.
17. Gao, C., Wang, G., Amack, J.D. and Mitchell, D.R. (2010) Oda16/Wdr69 is essential for axonemal dynein assembly and ciliary motility during zebrafish embryogenesis. *Dev. Dyn.*, **239**, 2190–2197.
18. Hou, Y., Qin, H., Follit, J., Pazour, G., Rosenbaum, J. and Witman, G. (2007) Functional analysis of an individual IFT protein: IFT46 is required for transport of outer dynein arms into flagella. *J. Cell Biol.*, **176**, 653–665.
19. Wakabayashi, K., Takada, S., Witman, G.B. and Kamiya, R. (2001) Transport and arrangement of the outer-dynein-arm docking complex in the flagella of *Chlamydomonas* mutants that lack outer dynein arms. *Cell Motil. Cytoskeleton*, **48**, 277–286.
20. Takada, S., Wilkerson, C.G., Wakabayashi, K.-I., Kamiya, R. and Witman, G.B. (2002) The outer dynein arm-docking complex: composition and characterization of a subunit (oda1) necessary for outer arm assembly. *Mol. Biol. Cell*, **13**, 1015–1029.
21. Casey, D.M., Inaba, K., Pazour, G.J., Takada, S., Wakabayashi, K.-I., Wilkerson, C.G., Kamiya, R. and Witman, G.B. (2003) DC3, The 21-kDa subunit of the outer dynein arm-docking complex (ODA-DC), is a novel EF-hand protein important for assembly of both the outer arm and the ODA-DC. *Mol. Biol. Cell*, **14**, 3650–3663.
22. Koutoulis, A., Pazour, G.J., Wilkerson, C.G., Inaba, K., Sheng, H., Takada, S. and Witman, G.B. (1997) The *Chlamydomonas reinhardtii* ODA3 gene encodes a protein of the outer dynein arm docking complex. *J. Cell Biol.*, **137**, 1069–1080.
23. Wirschell, M., Pazour, G., Yoda, A., Hirono, M., Kamiya, R. and Witman, G.B. (2004) Oda5p, a novel axonemal protein required for assembly of the outer dynein arm and an associated adenylate kinase. *Mol. Biol. Cell*, **15**, 2729–2741.
24. Wirschell, M., Olbrich, H., Werner, C., Tritschler, D., Bower, R., Sale, W.S., Loges, N.T., Pennekamp, P., Lindberg, S., Stenram, U. *et al.* (2013) The nexin-dynein regulatory complex subunit DRC1 is essential for motile cilia function in algae and humans. *Nat. Genet.*, **45**, 262–268.
25. Ishikawa, H. and Marshall, W.F. (2011) Ciliogenesis: building the cell's antenna. *Nat. Rev.*, **12**, 222–234.
26. Broekhuis, J.R., Leong, W.Y. and Jansen, G. (2013) Regulation of cilium length and intraflagellar transport. *Int. Rev. Cell Mol. Biol.*, **303**, 101–138.
27. Laurençon, A., Dubruille, R., Efimenko, E., Grenier, G., Bissett, R., Cortier, E., Rolland, V., Swoboda, P. and Durand, B. (2007) Identification of novel regulatory factor X (RFX) target genes by comparative genomics in *Drosophila* species. *Genome Biol.*, **8**, R195.
28. Göpfert, M.C. and Robert, D. (2003) Motion generation by *Drosophila* mechanosensory neurons. *Proc. Natl Acad. Sci. USA*, **100**, 5514–5519.
29. Han, Y., Kwok, B. and Kernan, M. (2003) Intraflagellar transport is required in *Drosophila* to differentiate sensory cilia but not sperm. *Curr. Biol.*, **13**, 1679–1686.
30. Sarpal, R., Todi, S., Sivan-Loukianova, E., Shirolikar, S., Subramanian, N., Raff, E., Erickson, J., Ray, K. and Eberl, D. (2003) *Drosophila* KAP interacts with the kinesin II motor subunit KLP64D to assemble chordotonal sensory cilia, but not sperm tails. *Curr. Biol.*, **13**, 1687–1696.
31. Briggs, L.J., Davidge, J.A., Wickstead, B., Ginger, M.L. and Gull, K. (2004) More than one way to build a flagellum: comparative genomics of parasitic protozoa. *Curr. Biol.*, **14**, R611–R612.
32. Bonnafe, E., Touka, M., AitLounis, A., Baas, D., Barras, E., Ucla, C., Moreau, A., Flamant, F., Dubruille, R., Couble, P. *et al.* (2004) The transcription factor RFX3 directs nodal cilium development and left-right asymmetry specification. *Mol. Cell. Biol.*, **24**, 4417–4427.
33. El Zein, L., Ait-Lounis, A., Morlé, L., Thomas, J., Chhin, B., Spassky, N., Reith, W. and Durand, B. (2009) RFX3 governs growth and beating efficiency of motile cilia in mouse and controls the expression of genes involved in human ciliopathies. *J. Cell Sci.*, **122**, 3180–3189.
34. Göpfert, M.C., Humphris, A.D.L., Albert, J.T., Robert, D. and Hendrich, O. (2005) Power gain exhibited by motile mechanosensory neurons in *Drosophila* ears. *Proc. Natl Acad. Sci. USA*, **102**, 325–330.
35. Kavlie, R.G., Kernan, M.J. and Eberl, D.F. (2010) Hearing in *Drosophila* requires TilB, a conserved protein associated with ciliary motility. *Genetics*, **185**, 177–188.
36. Kamikouchi, A., Inagaki, H.K., Effertz, T., Hendrich, O., Fiala, A., Göpfert, M.C. and Ito, K. (2009) The neural basis of *Drosophila* gravity-sensing and hearing. *Nature*, **458**, 165–171.

37. Kernan, M.J. (2007) Mechanotransduction and auditory transduction in *Drosophila*. *Pflugers Arch.*, **454**, 703–720.
38. Kramer-Zucker, A., Olale, F., Haycraft, C., Yoder, B., Schier, A. and Drummond, I. (2005) Cilia-driven fluid flow in the zebrafish pronephros, brain and Kupffer's vesicle is required for normal organogenesis. *Development*, **132**, 1907–1921.
39. Kishimoto, N., Cao, Y., Park, A. and Sun, Z. (2008) Cystic kidney gene seahorse regulates cilia-mediated processes and Wnt pathways. *Dev. Cell*, **14**, 954–961.
40. Sullivan-Brown, J., Schottenfeld, J., Okabe, N., Hostetter, C.L., Serluca, F.C., Thiberge, S.Y. and Burdine, R.D. (2008) Zebrafish mutations affecting cilia motility share similar cystic phenotypes and suggest a mechanism of cyst formation that differs from pkd2 morphants. *Dev. Biol.*, **314**, 261–275.
41. Melby, A.E., Warga, R.M. and Kimmel, C.B. (1996) Specification of cell fates at the dorsal margin of the zebrafish gastrula. *Development*, **122**, 2225–2237.
42. Cooper, M.S. and D'Amico, L.A. (1996) A cluster of noninvoluting endocytic cells at the margin of the zebrafish blastoderm marks the site of embryonic shield formation. *Dev. Biol.*, **180**, 184–198.
43. Essner, J., Amack, J., Nyholm, M., Harris, E. and Yost, H. (2005) Kupffer's vesicle is a ciliated organ of asymmetry in the zebrafish embryo that initiates left-right development of the brain, heart and gut. *Development*, **132**, 1247–1260.
44. Cao, Y., Park, A. and Sun, Z. (2010) Intraflagellar transport proteins are essential for cilia formation and for planar cell polarity. *J. Am. Soc. Nephrol.*, **21**, 1326–1333.
45. Jaffe, K.M. and Burdine, R.D. (2010) More than maintenance? A role for IFT genes in planar cell polarity. *J. Am. Soc. Nephrol.*, **21**, 1240–1241.
46. FlyBase (2002) The FlyBase database of the *Drosophila* genome projects and community literature. *Nucleic Acids Res.*, **30**, 106–108.
47. van Rooijen, E., Giles, R.H., Voest, E.E., van Rooijen, C., Schulte-Merker, S. and van Eeden, F.J. (2008) LRRC50, a conserved ciliary protein implicated in polycystic kidney disease. *J. Am. Soc. Nephrol.*, **19**, 1128–1138.
48. Kott, E., Duquesnoy, P., Copin, B., Legendre, M., Dastot-Le Moal, F., Montantin, G., Jeanson, L., Tamalet, A., Papon, J.-F., Siffroi, J.-P. *et al.* (2012) Loss-of-function mutations in LRRC6, a gene essential for proper axonemal assembly of inner and outer dynein arms, cause primary ciliary dyskinesia. *Am. J. Hum. Genet.*, **91**, 958–964.
49. Horani, A., Ferkol, T.W., Shoseyov, D., Wasserman, M.G., Oren, Y.S., Kerem, B., Amirav, I., Cohen-Cymberknoh, M., Dutcher, S.K., Brody, S.L. *et al.*. (2013) LRRC6 mutation causes primary ciliary dyskinesia with dynein arm defects. *PLoS ONE*, **8**, e59436.
50. Ahmed, N.T. and Mitchell, D.R. (2005) ODA16p, a *Chlamydomonas* flagellar protein needed for dynein assembly. *Mol. Biol. Cell*, **16**, 5004–5012.
51. Harder, S., Thiel, M., Clos, J. and Bruchhaus, I. (2010) Characterization of a subunit of the outer dynein arm docking complex necessary for correct flagellar assembly in *Leishmania donovani*. *PLoS Negl. Trop. Dis.*, **4**, e586.
52. Delaval, B., Bright, A., Lawson, N.D. and Doxsey, S. (2011) The cilia protein IFT88 is required for spindle orientation in mitosis. *Nat. Cell Biol.*, **13**, 461–468.
53. Parker, D.S. and Katsanis, N. (2011) Understanding cargo specificity in intraflagellar transport. *EMBO J.*, **30**, 2518–2519.
54. Zhao, C. and Malicki, J. (2011) Nephrocystins and MKS proteins interact with IFT particle and facilitate transport of selected ciliary cargos. *EMBO J.*, **30**, 2532–2544.
55. Kimmel, C.B., Ballard, W.W., Kimmel, S.R., Ullmann, B. and Schilling, T.F. (1995) Stages of embryonic development of the zebrafish. *Dev. Dyn.*, **203**, 253–310.
56. Vandesompele, J., De Preter, K., Pattyn, F., Poppe, B., Van Roy, N., De Paepe, A. and Speleman, F. (2002) Accurate normalization of real-time quantitative RT-PCR data by geometric averaging of multiple internal control genes. *Genome Biol.*, **3**, RESEARCH0034.
57. Carreira-Barbosa, F., Concha, M.L., Takeuchi, M., Ueno, N., Wilson, S.W. and Tada, M. (2003) Prickle 1 regulates cell movements during gastrulation and neuronal migration in zebrafish. *Development*, **130**, 4037–4046.
58. Amack, J. and Yost, H. (2004) The T box transcription factor no tail in ciliated cells controls zebrafish left-right asymmetry. *Curr. Biol.*, **14**, 685–690.
59. Thisse, C. and Thisse, B. (2008) High-resolution in situ hybridization to whole-mount zebrafish embryos. *Nat. Protoc.*, **3**, 59–69.
60. Enjolras, C., Thomas, J., Chhin, B., Cortier, E., Duteyrat, J.L., Soulavie, F., Kernan, M.J., Laurencon, A. and Durand, B. (2012) *Drosophila* chibby is required for basal body formation and ciliogenesis but not for Wg signaling. *J. Cell Biol.*, **197**, 313–325.
61. Sullivan-Brown, J., Bisher, M.E. and Burdine, R.D. (2011) Embedding, serial sectioning and staining of zebrafish embryos using JB-4 resin. *Nat. Protoc.*, **6**, 46–55.